

## Organic Field-Effect Transistors Using Di(2-thienyl)naphthodithiophenes as Active Layers

Yoshihito Kunugi,\* Kazuo Takimiya,<sup>†</sup> Kazuo Yamashita, Yoshio Aso,<sup>†</sup> and Tetsuo Otsubo<sup>†</sup>

Faculty of Integrated Arts and Sciences, Hiroshima University, 1-7-1 Kagamiyama, Higashi-Hiroshima 739-8521

<sup>†</sup>Graduated School of Engineering, Hiroshima University, 1-4-1 Kagamiyama, Higashi-Hiroshima 739-8527

(Received June 20, 2002; CL-020514)

Two isomeric di(2-thienyl)naphthodithiophenes, *anti*- and *syn*-DThNDTs, have been investigated as active materials of organic field-effect transistors (FETs). Field-effect mobilities of  $2\text{--}3 \times 10^{-4} \text{ cm}^2 \text{ V}^{-1} \text{ s}^{-1}$  were obtained for the *anti*-DThNDT film, while no obvious FET function was observed with the *syn*-DThNDT film.

Recently, organic field-effect transistors (OFETs) are receiving much attention because of their potential applications to flexible, light and small electronic devices.<sup>1,2</sup> A large number of small organic molecules and conjugated polymers such as pentacene,<sup>3</sup> oligothiophene<sup>4</sup> and poly(alkylthiophene)<sup>5</sup> can be used as active layers of the OFETs. It is worthy of note that the field-effect mobilities of  $1.5\text{--}3.1 \text{ cm}^2 \text{ V}^{-1} \text{ s}^{-1}$  reported for the single crystal p-type pentacenes are greater than those ( $0.1\text{--}1 \text{ cm}^2 \text{ V}^{-1} \text{ s}^{-1}$ ) for a-Si.<sup>1,3</sup>

We have recently synthesized naphthodithiophene derivatives, which are new types of heteroarene isoelectronic with pyrene.<sup>6-8</sup> In this work, isomeric 2,6-di(2-thienyl)naphtho[1,8-bc : 5,4-b'c']dithiophene (*anti*-DThNDT) and 2,5-di(2-thienyl)naphtho[1,8-bc : 5,4-b'c']dithiophene (*syn*-DThNDT) were studied as active materials of the OFETs. The *anti*-DThNDT is a linear and plane molecule which has a  $C_2$  symmetry axis, while the *syn*-DThNDT is a bent molecule though there is a  $C_2$  axis as well as a symmetry plane. Electronic absorption maxima of the *anti*- and *syn*-DThNDT in tetrahydrofuran are 519 and 444 nm, respectively, indicating that the *anti*-DThNDT has narrow HOMO-LUMO energy-gap compared with the *syn*-DThNDT.<sup>8</sup>

The *anti*- and *syn*-DThNDTs were synthesized as described already.<sup>8</sup> OFETs were fabricated on heavily doped  $n^+$ -Si (100) wafers with a 220 nm thermally grown  $\text{SiO}_2$ . The DThNDTs (50–100 nm thick) were thermally deposited onto the  $\text{SiO}_2/\text{Si}$  substrate, and succeeding Au films (100 nm) as drain and source electrodes were deposited on the organic layer through a shadow mask (Figure 1). For a typical device, the drain-source

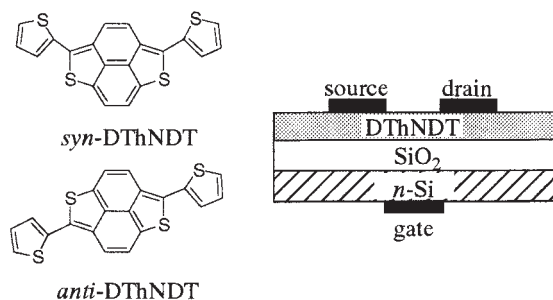


**Figure 1.** Chemical structures of organic materials used and the device structure of the OFET.

channel length and width are  $50 \mu\text{m}$  and  $2 \text{ mm}$ , respectively. Characteristics of a drain current ( $i_d$ ) versus drain voltage ( $V_d$ ) of the OFET devices were measured with an ADVANTEST R6245 power supply under dry  $\text{N}_2$  atmosphere. The field-effect mobilities ( $\mu_{\text{FET}}$ ) were calculated in the saturation regime using the equation (1).

$$i_d = \frac{WC_i}{2L} \mu_{\text{FET}} (V_g - V_t)^2 \quad (1)$$

where  $W$  and  $L$  are the channel width and length, respectively.  $C_i$  is the capacitance per unit area of the  $\text{SiO}_2$ ,  $V_g$  the gate voltage and  $V_t$  the threshold voltage which can be calculated from a plot of  $(i_d)^{1/2}$  vs  $V_g$ . X-ray diffraction (XRD) of the organic thin films on  $\text{SiO}_2/\text{Si}$  substrate was measured with a Maxscience M18XHF diffractometer. UV-Vis spectra and AFM images of the organic thin films were obtained by using a Shimadzu UV-3101PC spectrometer and Shimadzu SPM-9500 microscope, respectively. All the measurements were conducted at room temperature.

The thin film of the *anti*-DThNDT is shiny and red-purple, while the *syn*-DThNDT film is rough and yellow. The optical absorption maxima of *anti*- and *syn*-DThNDT films are 480 nm and 412 nm, respectively. XRD of the *anti*-DThNDT film on  $\text{SiO}_2/\text{Si}$  substrate exhibited a  $d$  spacing of  $13.40 \text{ \AA}$ . This value is consistent with the  $a$  axis of the single-crystal unit-cell ( $a$ :  $13.33 \text{ \AA}$ ,  $b$ :  $3.93 \text{ \AA}$ ,  $c$ :  $15.26 \text{ \AA}$ ).<sup>8</sup> On the other hand, any significant peak was not observed with the *syn*-DThNDT film, indicating that the film is amorphous.

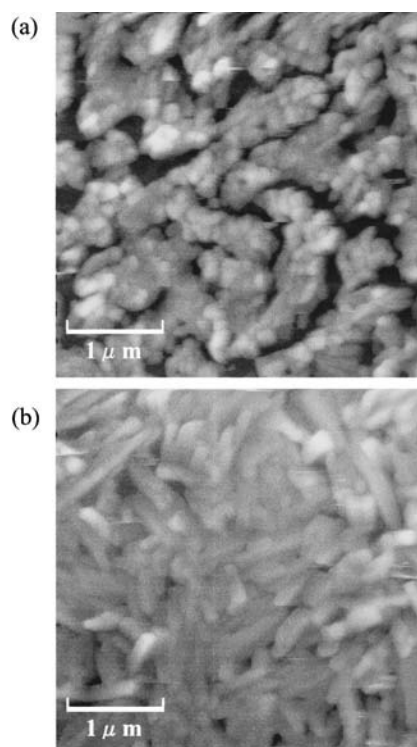
Figure 2 shows AFM images of the (a) *syn*- and (b) *anti*-DThNDT films (100 nm) on  $\text{SiO}_2/\text{Si}$  substrate. For the *syn*-DThNDT film, large grain (about  $1\text{--}2 \mu\text{m}$  length) consists of cohered small grain (diameter =  $0.1\text{--}0.2 \mu\text{m}$ ) and  $\text{SiO}_2/\text{Si}$  substrate is not wholly covered with *syn*-DThNDT. In the case of the *anti*-DThNDT film,  $\text{SiO}_2/\text{Si}$  substrate is fully covered with needle-like crystals (diameter =  $0.2\text{--}0.3 \mu\text{m}$ ).

Figure 3 shows a typical plot of the  $i_d$  vs  $V_d$  at various  $V_g$  for the OFET based on *anti*-DThNDT. The channel conductance increases as  $V_g$  becomes more negative, meaning that the *anti*-DThNDT film behaves as a p-type semiconductor. The  $\mu_{\text{FET}}$  estimated for the *anti*-DThNDT film was  $2\text{--}3 \times 10^{-4} \text{ cm}^2 \text{ V}^{-1} \text{ s}^{-1}$ . On the other hand, no obvious FET function was observed with the *syn*-DThNDT film. The  $i_d$  observed was less than  $1 \text{ nA}$  when the  $V_d$  and  $V_g$  were varied in the range from 0 to  $-100 \text{ V}$ , respectively. This is consistent with the AFM image described above, indicating the formation of the island-like film for *syn*-DThNDT.

The effective carrier mobility ( $\mu_{\text{eff}}$ ) across two grains in the polycrystalline film is given by the equation (2).

$$\frac{1}{\mu_{\text{eff}}} = \frac{1}{\mu_c} + \frac{1}{\mu_{\text{gb}}} \quad (2)$$

where,  $\mu_c$  and  $\mu_{\text{gb}}$  are carrier mobilities in the crystal grain



**Figure 2.** AFM images of the (a) *syn*- and (b) *anti*-DThNDT films (100 nm) on SiO<sub>2</sub>/Si.

(intragrain mobility) and across the grain-boundary, respectively. Usually,  $\mu_c$  is larger than  $\mu_{gb}$ , so that the overall mobility for the polycrystalline film increases with the decrease of the number of grain-boundaries and the distance between the grains. A similar consideration is applicable to the present case. Namely, the charge transport is predominated by the intergrain transport. Further studies are in progress to improve the  $\mu_{FET}$  by molecular design.

In summary, the sublimed *anti*-DThNDT film behaves as a p-channel semiconductor in the OFET and the  $\mu_{FET}$  calculated in the saturation regime is  $2\text{--}3 \times 10^{-4} \text{ cm}^{-2} \text{ V}^{-1} \text{ s}^{-1}$ . The FET based on *syn*-DThNDT did not work sufficiently. The results are attributed to the difference in morphology between the *anti*- and *syn*-DThNDT films. The XRD and AFM indicate that *anti*-DThNDT forms a highly packed film, but *syn*-DThNDT forms a porous film having grain-gaps (0.1–0.2  $\mu\text{m}$ ). The plane and symmetric molecules such as *anti*-DThNDT are suitable for the active materials in the OFETs.

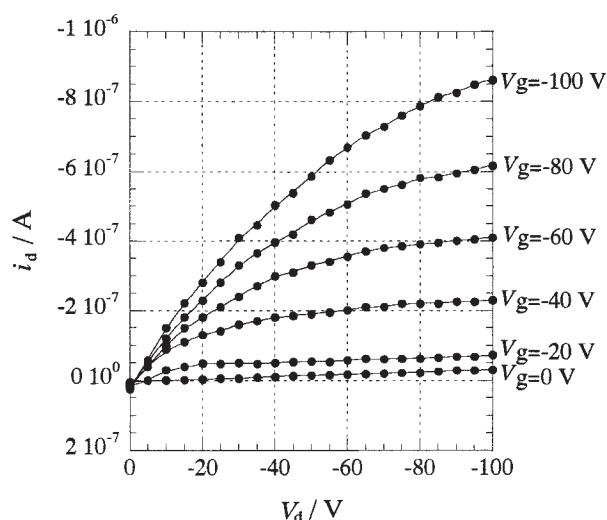


**Figure 3.**  $i_d$  vs  $V_d$  curves at different gate biases for the OFET device using the *anti*-DThNDT film as an active layer.

This work was supported by Industrial Technology Research Grant Program in 2001 from NEDO of Japan (01A26005a) and Grants-in-Aid for Scientific Research from the Ministry of Education, Science, Sports and Culture of Japan (13750761). We thank Professors S. Yamanaka, K. Inumaru and H. Fukuoka (Hiroshima University) for the measurements of XRD. We also thank Mr. H. Murakami (Hiroshima University) for experimental helps of the Si-wafer treatments.

#### References

- 1 C. D. Dimitrakopoulos and L. R. L. Malenfant, *Adv. Mater.*, **14**, 99 (2002).
- 2 J. H. Schon, H. Meng, and Z. Bao, *Nature*, **413**, 714 (2001).
- 3 a) Y.-Y. Lin, D. J. Gundlach, S. Nerson, and T. N. Jacson, *IEEE Electron Devices Lett.*, **18**, 606 (1997). b) J. H. Schon, *Synth. Met.*, **122**, 157 (2001).
- 4 H. E. Katz, A. J. Lovinger, and J. G. Laquindanum, *Chem. Mater.*, **10**, 457 (1998).
- 5 H. Sirringhaus, N. Tessler, and R. H. Friend, *Science*, **280**, 1741 (1998).
- 6 K. Takimiya, F. Yashiki, Y. Aso, T. Otsubo, and F. Ogura, *Chem. Lett.*, **1993**, 365.
- 7 K. Takimiya, T. Otsubo, and F. Ogura, *J. Chem. Soc., Chem. Commun.*, **1994**, 1859.
- 8 K. Takimiya, K. Kato, Y. Aso, F. Ogura, and T. Otsubo, *Bull. Chem. Soc. Jpn.*, **75**, 1795 (2002).